Proceedings of the Thirty-second (2022) International Ocean and Polar Engineering Conference **www.isope.org**
Shanghai, China, June 5–10, 2022

ISBN 978-1-880653-81-4; ISSN 1098-6189

A Novel Energy Harvesting Mechanism and its Design Methodology for Underwater Gliders Using Thermal Buoyancy Engines

Hongbo Hou, Weichao Shi, Abel Arredondo Galeana
Naval Architecture, Ocean and Marine Engineering, University of Strathclyde
Glasgow, UK
Yang Song
School of Mechanical Engineering, Tianjin University
Tianjin, China

ABSTRACT

Underwater gliders are becoming popular in ocean exploration. However, the main development limitation of underwater gliders is still around energy. This paper proposes a new-type energy harvesting mechanism and explores its design methodology for the gliders using thermal buoyancy engines. With the temperature difference in the ocean, the thermal buoyancy engine changes the buoyancy of the glider and drives the glider to ascend and descend through the water and drive a turbine behind to harvest energy. Based on this harvesting mechanism, firstly, a new-type thermal engine with high ballast capacity is developed with patent applied. Secondly, a dedicated turbine design and optimization method based on modified Blade Element Momentum (BEM) theory has been developed to maximize the energy harvesting capability.

KEY WORDS: Underwater gliders; energy harvesting mechanism; thermal buoyancy engine; turbine; BEMT.

INTRODUCTION

Recently, the underwater glider has become one of the major workforces in ocean exploration because of its long endurance and low operational cost. The glider of this work is powered by a buoyancy engine, which can generate the buoyancy change to drive the glider to ascend and descend in the water. Horizontal forces are generated through hydrofoils, allowing the underwater glider to move in a sawtooth trajectory, which is shown in Fig.1.

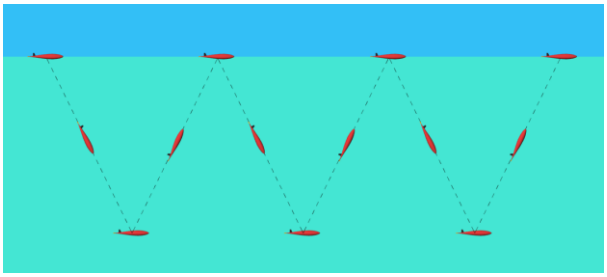

Fig.1 the sawtooth trajectory of underwater glider

Companies and organizations have already developed several commercial underwater gliders with electrical buoyancy engines, such as Slocum(Jones, Allsup, & DeCollibus, 2014), Seaglider (Eriksen et al., 2001), Spray (Sherman, Davis, Owens, & Valdes, 2001). To make the glider a permanent ocean resident, thermal gliders are proposed to use ocean thermal energy to drive the thermal buoyancy engine and drive the gliders up and down. As a good alternative to the electrical buoyancy engine which relies on battery power, the thermal buoyancy engine can harvest thermal energy of the ocean to increase the voyage of the glider by 3-4 times (Russ E Davis, Eriksen, Jones, & vehicles, 2002). For example, the pioneer Slocum glider with a thermal buoyancy engine developed by the Webb Research Corporation reached 40000km (Webb, Simonetti, & Jones, 2001).

However, thermal gliders are still limited by the battery power which provides energy for their onboard payloads and attitude control systems. On the other hand, both electrical and thermal gliders are limited by the slow speed, maximum 1knot, which often requires additional thrusters if high-speed cruising is needed. Therefore, conversion between thermal energy and electrical energy is needed. Current developments focus on hydraulic-based systems, which use a mini generator in the high-pressure oil pipeline trying to recover the energy while ballasting and de-ballasting. In 2016, SOLO-TREC was developed based on this principle (Chao, 2016). The Teledyne Webb Research consortium built the Slocum Thermal E-Twin with a similar power generation system for developing global class gliders (Jones et al., 2014). The advantage of this kind of power generation system is that it is simple and compact. The disadvantage is that it is limited in energy output. For example, the energy yield of the Slocum-TREC glider with 10kg PCM based on this principle is around 6.5KJ per working cycle(Wang, Yang, & Wang, 2020). At the same time, the hydraulic generator has to work in high pressure and low volume oil loop which results in low efficiency and high failure rate.

This research proposes a new type of energy harvesting mechanism which can be applied to thermal underwater gliders aiming for high energy yield. The mechanism uses a thermal buoyancy engine and a foldable power generation turbine. When the glider is in the power-generating mode, the thermal buoyancy engine can use the thermal energy to change its buoyancy to drive the glider vertically. During the ascend and descend, the foldable turbine behind the hull will open and

start spinning to harvest energy. To maximize the power output of the energy harvesting system with the thermal engine and the turbine, this study designs a new-type thermal engine with high ballast capacity in order to provide a large driving force. Followingly, this study develops a mathematical model based on Blade Element Momentum Theory (BEMT) to design and optimize the turbine.

NEW TYPE OF ENERGY HARVESTING MECHANISM

As mentioned above, this research proposes a new-type energy harvesting mechanism. To balance the energy-efficient gliding and the energy harvesting, the glider is designed to have two operating modes: the gliding mode and the power generation mode. In the gliding mode, the glider is driven by the thermal buoyancy engine to move in a saw-tooth trajectory. In this condition, the thermal buoyancy engine uses part of its ballast capacity to allow the vehicle to glide in an energy-efficient manner. To minimise the resistance while gliding, the turbine behind folds, as shown in Fig.2.

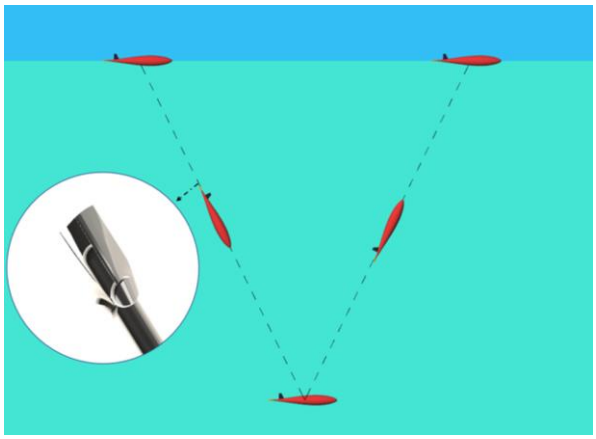

Fig.2 The gliding mode

When the underwater glider turns into power generation mode, the thermal buoyancy engine will harvest thermal energy and use its maximum ballast capacity to drive the underwater glider moving at its highest speed vertically. In the meantime, the foldable turbine unfolds to harvest energy by rotating and driving an electric generator in the glider hull, as shown in Fig.3.

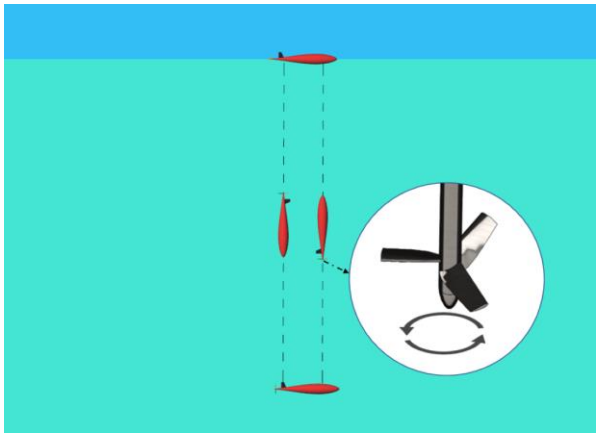

Fig.3. Power generation mode

As it can be expected in this process, the efficiency of the thermal buoyancy engine and the turbine will directly affect the amount of energy that is harvested. Therefore, improving the operation of both the engine and the turbine is key to the success of this technology.

THERMAL BUOYANCY ENGINE FOR ENERGY HARVESTING

The temperature of the seawater drops rapidly from 20-30°C to generally 4°C with the water depth in the ocean due to the ocean thermocline (Kong, Ma, & Xia, 2010). With the temperature difference between the surface and the deep sea, the ocean thermal energy is formed (Ma, Wang, Wang, & Yang, 2016). The thermal buoyancy engine is a device that can harvest ocean thermal energy by phase change material (PCM). The device uses the thermal energy to change its buoyancy so that to drive the glider up and down in the ocean (Javaid, Ovinis, Nagarajan, & Hashim, 2014; Yang, Wang, Ma, & Wang, 2016). As the engine drives the power generation system, the thermal buoyancy engine will directly determine the upper limit of the harvestable kinetic energy. However, the previous thermal buoyancy engine design is more towards driving gliders to perform the gliding motion instead of energy harvesting. It is generally designed to have a small capacity and for lower velocity, like 0.5 m in the water. But to provide more kinetic energy input to the turbine, this paper proposes a new-type thermal buoyancy engine that can increase the ballast capacity without increasing the volume of PCM.

Traditional Thermal Buoyancy Engine

Before introducing the new-type thermal engine, the principle of the traditional thermal engine will be introduced. Fig.4 shows the schematic of the traditional thermal engine system(Webb et al., 2001). Chamber (1) is the heat transfer, the working fluid in it is the phase change material (PCM) which can expand and squeeze the hydraulic oil into the chamber (2) when it harvests thermal energy and melts. Chamber (2) is a mechanical energy storage accumulator with high-pressure N2 in it. According to the working principle of the thermal engine, the whole working cycle can be divided into 4 steps. In step (1), the PCM in the heat transfer continues to melt and squeeze the oil into the accumulator, the check valve can prevent the oil backflow. In step (2), the oil in the external bladder is squeezed into the inner bladder by atmospheric pressure when the 3-way valve opens, the buoyancy decreases, and the glider descends. with the increase of the depth, the temperature is falling rapidly. The liquid PCM starts to solidify and contrast, the oil in the internal bladder flow into the heat transfer. In step (3), the glider reaches the pre-programmed depth, the 3-way valves open and the oil in the accumulator is pushed into the external bladder, the buoyancy increase and the AUV starts ascending. In step (4). The AUV reaches the sea surface, next circle starts(Webb et al., 2001).

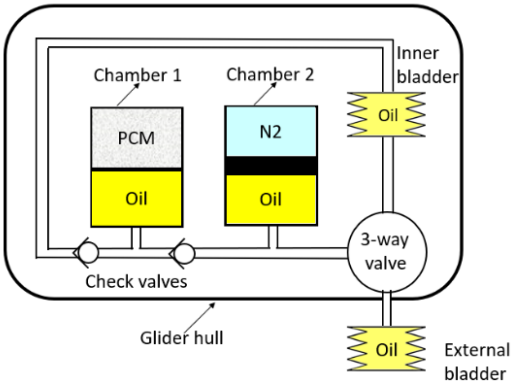

Fig.4 Schematic of the traditional thermal engine system

The advantage of this type of heat engine is its simple structure and

reliability. However, its disadvantage is also prominent that the ballast force is very limited. For example, the Slocum thermal E-twin with two heat transfers can only provide about 1000 cc working pressurized oil or 10 N buoyancy force(Jones et al., 2014). The reason is that the mass of phase change material (PCM) that can be accommodated in the glider is limited and the PCM has a low expansion rate, normally less than 10%. The limited ballast force offered by the traditional thermal engine cannot provide the turbine behind the hull with enough kinetic energy.

The New-type Buoyancy Engine Of This Study

To provide more kinetic energy to the turbine in the energy harvest mechanism, this paper proposes a new-type thermal buoyancy engine with patent applied which is specialized to amplify the ballast capacity without increasing the mass of PCM(Shi, Hou, Xu, & Mehmet, 2022). The principle of the new-type buoyancy engine in this paper is to fully use the high pressure that the PCM can generate by increasing the working pressure of PCM in the heat transfer and converting the high pressure of the PCM into the low working pressure of underwater glider.

In a traditional buoyancy engine, the working pressure of PCM is very low compared to the highest pressure the melting PCM can generate. The working pressure of PCM is only about 11 to 12 MPa (Ma et al., 2016). In the meantime, the maximum pressure generated by melting PCM can be much higher than the working pressure of the underwater glider. For example, the volumetric expansion rate of paraffin wax can reach 9 % in the phase change process when the pressure is 60 Mpa (Klintberg, Karlsson, Stenmark, Schweitz, & Thornell, 2002). According to the research of Falcão(2016), when the n-pentadecane is used as the PCM in the heat transfer, its working pressure needs to reach 90Mpa to get the highest thermodynamic efficiency(Falcão Carneiro & Gomes de Almeida, 2016). It means that the pressure of melting PCM or the pressure in the accumulator is too low for the PCM to release all its potential power.

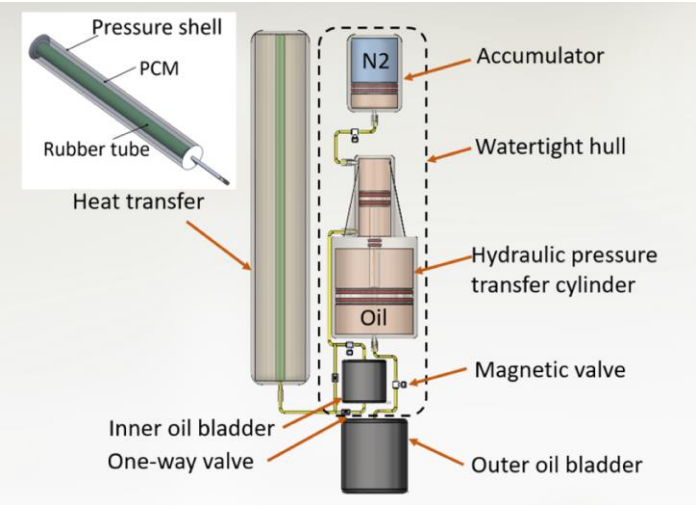

Fig.5 the schematic of the new-type thermal buoyancy engine

This property of PCM gives inspiration to this study. In this work, a new-type thermal engine is invented to fully use the high pressure that the PCM can generate to amplify the ballast capacity of the engine. The whole idea can be divided into 2 steps. The first step is to increase the pre-charge pressure(P_P) in the accumulator which equals the working pressure of PCM in heat transfer according to the thermodynamic properties of PCM. The higher pre-charge pressure(P_P) will enable the PCM to work in the higher thermodynamic efficiency. The second step is to use a hydraulic pressure transfer cylinder which is shown in Fig.5 to convert the high pre-charge pressure(P_P) of oil in the accumulator to low working pressure in the outer bladder. The hydraulic pressure transfer cylinder in this study consists of a high-pressure double-acting cylinder with a small cross-sectional area, a single-acting low-pressure cylinder with a large cross-sectional area, and a hydraulic rod connecting the pistons in the two cylinders. When the hydraulic pressure transfer cylinder is transferring the oil from higher pressure to low pressure, it will also amplify the oil volume change in the high-pressure cylinder to the oil volume change in the low-pressure cylinder. In other words, the hydraulic pressure transfer cylinder is a ballast force amplifier. The buoyancy magnification (M_b) is the ratio between the cross-sectional area of the low-pressure cylinder to the cross-sectional area of the high-pressure cylinder. With the same amount of PCM, the new-type buoyancy engine can amplify the buoyancy change by M_b times in order to provide more kinetic energy to the turbine. The schematic of the new-type thermal buoyancy engine is shown in Fig.5.

THE DESIGN AND OPTIMIZATION OF THE TURBINE BY ESTABLISHING A MATHEMATICAL MODEL

The turbine is used for harvesting kinetic energy provided by the thermal buoyancy engine and converting the kinetic energy into electricity, so, the geometry of the turbine will directly determine how much electricity the system can generate. To design and optimize a turbine geometry for maximizing the energy yield, this paper establishes a mathematical model based on Blade Element Momentum Theory (BEMT). The mathematical model can also be used to estimate the power generation capacity of the system. According to the special working condition of the turbine in this work, the BEMT will be modified according to the wake distribution and the Reynolds number (Re) of the turbine before establishing the whole mathematical model.

Modified BEMT In This Study

The principle of traditional BEMT

The Blade Element Momentum Theory (BEMT) is the combination of the blade element theory and the momentum theory. The blade element theory divides the turbine blade into several individual foil elements. Assuming forces acting on the blade elements are only determined by the lift and drag coefficients of the foil (Bangga et al., 2018). The momentum conservation theory can be used to calculate the change of flow momentum and angular momentum around the blade and equate them to calculate the load on the blades. (Liu & Janajreh, 2012).

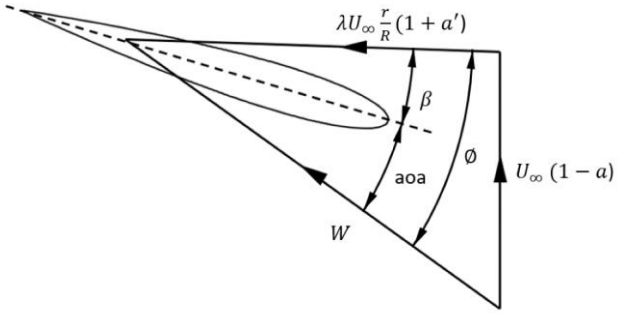

Fig.6 Velocities relating to the turbine blade

The BEMT can be used to design a turbine. The velocities in BEMT relating to the turbine blade are shown in Fig.6, the a is the axial induction factor which indicates a reduction percentage of upstream flow

velocity in front of the turbine. According to Betz limit, a turbine can harvest the maximum power when the a equals $\frac{1}{3}$ because the highest extractable power for a turbine can be achieved by reducing the flow velocity through the turbine plane to two-thirds of its upstream value(Ragheb & Ragheb, 2011). With the optimal a, the tangential induction factors (a') can be calculated by Eq.1.

$$a' = \frac{a(1-a)}{\lambda^2 \mu^2} \quad (1)$$

Where the λ is the tip speed ratio (TSR). The μ is the ratio of the local radius to the total radius ($\frac{r}{R}$).

After getting the a and the a', the local inflow angle ($\emptyset$) can be calculated by Eq.2:

$$tan\,\emptyset = \frac{1-a}{\lambda\mu(1+a')} \quad (2)$$

Then, the optimal twist angle of the blade element can be calculated by Eq.3

$$\beta = \phi - aoa \quad (3)$$

Where the aoa is the angle of attack of the foil with the highest lift-to-drag ratio.

According to BEM theory, torque at each radius calculated from the blade element theory equals the torque calculated from the momentum theory, formulating this relationship can get Eq.4. With Eq.4, the optimal chord length can be calculated.

$$\frac{W^2}{U_\infty^2} N \frac{C}{R}(C_L sin\emptyset - C_d\, cos\,\emptyset) = 8\pi\lambda\mu^2 a' \quad (1-a) \quad (4)$$

Where the C is the chord length, the C_L is the lift coefficient, the C_d is the drag coefficient, the N is the blade number, the U_∞ is the incoming flow velocity.

The BEMT can also be used to analyze the hydrodynamic performance of a turbine. The analysis part of BEMT will use iteration to determine the a and a' of the blade element to calculate the load on the foil. In the first step, the a and a' will be set as zero, then the inflow angle will be calculated by Eq.5.

$$tan\,\emptyset = \frac{1-a}{\lambda\mu(1+a')} \quad (5)$$

After this, the angle of attack (AOA) will be calculated which will be used to find the lift coefficient (Cl) and drag coefficient (Cd) of the foil in the next step. With the Cl and Cd, the normal coefficient (C_n) and the tangential coefficient (C_t) of the foil will be calculated by Eqs. 6~7.

$$C_n = C_L\, cos\,\emptyset + C_D\, sin\,\emptyset \quad (6)$$

$$C_t = C_L\, sin\,\emptyset - C_D\, cos\,\emptyset \quad (7)$$

With the C_n and C_t, the axial and tangential induction factors can be determined using the Eqs. 8~9 after multiple iterations:

$$a = \frac{1}{\frac{4sin^2\phi}{\sigma_r C_n}+1} \quad (8)$$

$$a' = \frac{(1-a)\sigma_r C_t}{4\lambda\mu sin^2\phi} \quad (9)$$

Where the σ_r is the chord solidity of the turbine.

Modifications to traditional BEMT

Unlike the typical application condition of BEMT, the working condition of the turbine in this study has two characteristics. The first one is that the blade elements may work in the strong wake behind the hull. The second one is that the blade elements may work in a very low Reynolds number (Re). These two characteristics will influence the design and analysis of BEMT. According to these two points, the mathematical model in this paper modified the traditional BEMT.

The first modification is the wake modification which makes each blade element work under the optimal angle of attack and enables the analysis part of BEMT to reflect the existence and influence of the wake, the traditional BEMT will be modified according to the wake distribution from CFD simulation for the selected glider hull in this study. The wake distribution behind the underwater glider from CFD simulation in this work is shown in Fig.7.

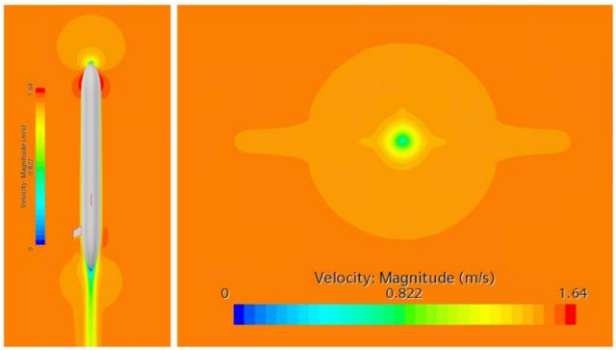

Fig.7 the typical wake distribution behind the underwater glider

It can be observed that the wake is approximately axial symmetric because the wings of the underwater glider have very limited influence on the wake. According to this property, the approximate axial symmetric wake distribution is simplified as complete axial symmetric. Then, the TSR in the design and analysis part of BEMT will be replaced by the equivalent TSR ($TSR_{equivalent}$) at each different radius which is shown in Eq.10.

$$TSR_{equivalent} = \frac{TSR \times U_\infty}{V_{wake}} \quad (10)$$

Where the V_{wake} is the flow velocity in the wake behind the glider at each radius from the CFD simulation.

The reason for modifying the traditional BEMT in this way is that the blade elements in the wake are equivalent to operating at higher TSR due to the presence of stronger wakes in this research. In the design part of BEMT, the equivalent TSR will enable blade elements to work under the optimal angle of attack. In the analysis part of BEMT, the modification enables the BEMT to reflect the existence and influence of the wake. With the Equivalent TSR, the a the a' and the AOA of the foil in the wake can be analyzed.

The second modification is the low Re modification. In the traditional BEMT, the lift coefficient (Cl) and the drag coefficient (Cd) are two curve functions about the angle of attack (AOA) and do not consider the influence of Reynolds number (Re) on hydrodynamic performance. In this work, this approach may no longer be appropriate. Considering the low moving speed of the whole system and the influence of the wake, the turbine blades sometimes work in a very low Reynolds number (Re)

which may be below 50,000. In this range, the hydrodynamic performance of the blade element will deteriorate sharply and be sensitive to the Re(Deters, Ananda, & Selig, 2014; Li, 2013). To consider the influence of Reynolds number (Re) on hydrodynamic performance of foil, in the design and analysis part of BEMT in this work, the hydrodynamic performance of the foil, including coefficient (Cl) and drag coefficient (Cd), will be two surface functions about Angle of attack (AOA) and Reynolds number (Re). Fig.8 shows how Re can influence the lift-to-drag ratio of the NACA 0015 foil used in this work. The surface functions of Cl and Cd are obtained by calculating and interpolating the hydrodynamic performance of the NACA 0015 under different Re and AOA by the software Xfoil.

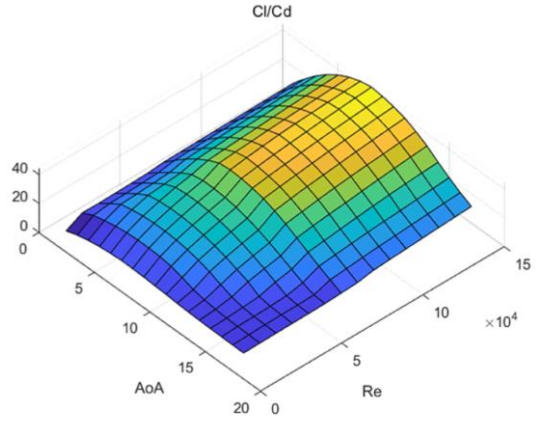

Fig.8 the lift-to-drag ratio of NACA 0015

In the analysis part, it is relatively simple to consider how the Reynolds number influences the hydrodynamic performance of blade elements since the turbine geometry has been determined. However, in the design part, the geometry of the turbine is unknown, so the Re is unknown. In this work, iteration will be used to determine the Re and final geometry. The process of iteration is shown in Fig.9.

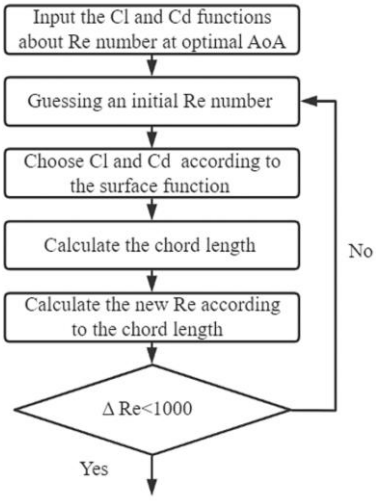

Fig.9: The iteration to determine the geometry of a turbine

To improve the accuracy of the BEMT, several existing engineering corrections also have been implemented in this work. The corrections include Shen's tip loss correction(Shen, Mikkelsen, Sørensen, & Bak, 2005), turbulent wake state correction(Buhl, 2005), the 3D correction(Chaviaropoulos & Hansen, 2000).

Mathematical Model For The Energy Harvest System Based On Modified BEMT

After having the modified BEMT, the next step is to construct the overall mathematical model to optimize the turbine geometry and estimate the maximum energy yield of the power generation system. The whole math model can be divided into the 18 steps whose flow chart is shown in Fig.10. The specific content of this flowchart will be described detailedly in the following content.

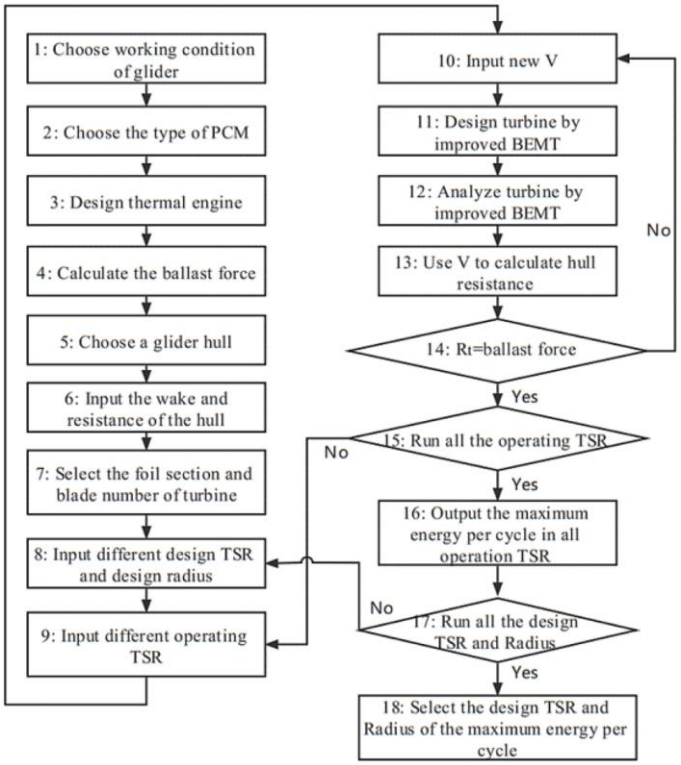

Fig.10 the flow chart of the math model

Step 1：Input the working environment of the glider, including the working depth of the glider (d_w), the water temperature of the sea surface(T_h) and water temperature of working depth (T_l) which are 1000 meters, 28 ℃, and 4 ℃ respectively (Ma et al., 2016).

Step 2：Select the type of PCM in the thermal engine, different PCMs have different PVT relationship which relates to the pressure(P), volume(V), and temperature(T) of the material. In this case, the PCM is n-pentadecane. The PVT relationship of n-Pentadecane proposed by Falcão is used, which is shown in Eq.11.(Falcão Carneiro & Gomes de Almeida, 2016).

$$V_{PCM_S} = 1.198 - \left(\frac{1}{55}\right)\left(P_{PCM} * 0.0143 - 0.0408 * (T_{PCM} + 5.5)\right)$$
$$V_{PCM\_T} = 1.249 - \left(\frac{1}{1023.9}\right)\left(P_{PCM} * 1.1 - 11 * (T_{PCM} - 10)\right)$$
$$\left(V_{PCM\_L} = 1.3195 - (\frac{1}{300})(P_{PCM} * 0.1817 - 0.2733 * (T_{PCM} - 30)\right) \quad (11)$$

Where V_{PCM_S}, V_{PCM_T}, V_{PCM_L} are the volume of PCM in solid, transition, and liquid phases respectively.

Step 3: Design thermal buoyancy engine, including the volume of phase change material(V_{pcm}) in the thermal engine, pre-charge pressure(P_P) in the accumulator, the buoyancy magnification (M_b), the pressure in the hull (P_{inner}). In this paper, V_{pcm} is 12 liters (about 10kg PCM) which is compatible with existing gliders (Falcão Carneiro & Gomes de Almeida, 2016). The P_P is selected according to the thermodynamic properties of the phase change material (PCM). According to Falcão's research, the efficiency of the thermal engine will reach a peak when the pressure of n-Pentadecane is 90 Mpa. Higher pre-charge pressure will cause the volume change of PCM to decrease, resulting in less work(Falcão Carneiro & Gomes de Almeida, 2016). Since the pressure in working water depth (d_w) is 10 Mpa, the P_P is 90 Mpa, so the theoretical buoyancy magnification (M_b) can be 9 without considering energy loss of the hydraulic system. Roughly considering the energy loss of the hydraulic system, the $M_b$is set as 8.5. In other word, in the new-type thermal buoyancy engine, the ratio of the cross-sectional area of the low-pressure cylinder to the cross-sectional area of high-pressure cylinder is 8.5. Air pressure in the hull (P_{inner}) is used to squeeze the oil in the inner bladder back to the heat transfer when the PCM is solidifying, and it can affect the volume of solid PCM at low temperature, in this case, the P_{inner} is set as 0.1 Mpa.

Step 4：Calculate the ballast force the thermal buoyancy engine can provide. With the equation in the second step, the unit volume of PCM in high temperature (V_{PCM_L}) and in low temperature (V_{PCM_S}) can be calculated by inputting P_P, T_h, P_{inner}, T_l to the Eq.11. Since a half of the buoyancy provided by the thermal engine is used to drive the glider downward and a half drives the glider upward, the ballast force is half of the buoyancy generated by the thermal engine, which is shown in Eq.12. With Eq.12, the ballast force is 25 N in this case.

$$Ballast\ force = V_{pcm} * \frac{V_{PCM_L}}{V_{PCM_S}} * M_b * density_{water} * g/2 \quad (12)$$

Step 5: Select a glider hull, in this work, a typical glider hull is chosen, the diameter is 19 cm, and the length is 2 meters. The geometer of the glider is shown in Fig.11

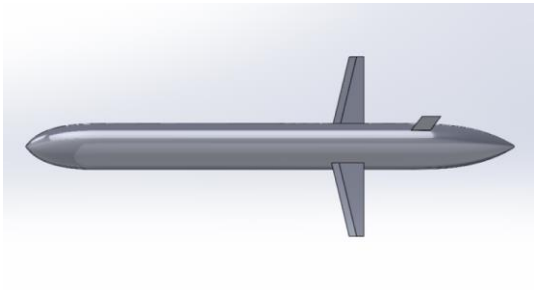

Fig.11 the geometry of the glider in this study

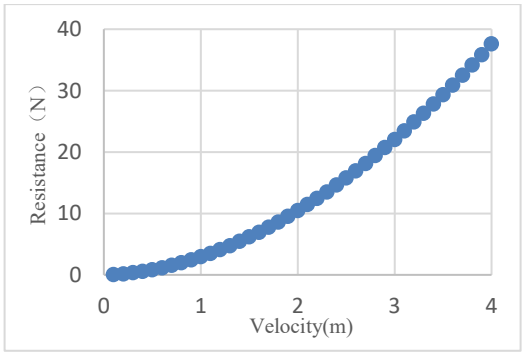

Fig.12 The hull resistance from CFD simulation

Step 6: Input the wake distribution and resistance of the hull from the CFD simulation. This work uses the CFD software STAR CCM+ to simulate this glider hull at different velocities. The result will provide the wake distribution of 10 cm after the glider which is shown in Fig.7 and the glider hull resistance in different velocities which is shown in Fig.12. Then, the wake distribution and resistance will be input into the mathematical model in functional form.

Step 7： Select the foil section and blade number of the turbine, the case in this paper selects NACA0015 as the foil section which is shown in Fig.13. The blade number is 3。

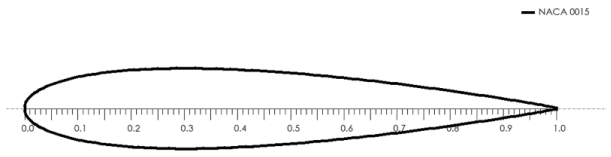

Fig.13 the NACA 0015 foil section

Step 8: Import different design TSRs and radii. In this case, the TSR is from 2 to 6 and the radius is from 0.06 to 0.15 m.

Step 9: Import different operating TSR. Every operating TSR of a specific turbine has its own Cp and Ct, then, the mathematical model will select the operating TSR with the most balanced Ct and Cp to harvest the most energy.

Step 10: Input the possible operating speed range from V_1 to V_n. As mentioned above, the BEMT in this mathematical model will consider the influence of the Re number on the hydrodynamic performance of the turbine. In other words, the Ct of the turbine will change with the glider speed, in the meantime, glider speed will change with Ct because of the change of thrust. To find out the actual running speed, this mathematical model will do multiple calculations to find the real operation speed of a turbine.

Step 11：The ith speed V_i in the speed range is received by modified BEMT, the modified BEMT will calculate the Reynolds number Re_i of each blade element, then, use the Re_i, design TSR, design radius to design a turbine by iteration.

Step 12：Input the geometry of the turbine designed in step (11) to the analysis part of the modified BEMT. The mathematical model will analyze the turbine's power coefficient (Cp_i), thrust coefficient (Ct_i), thrust (T_{t_i}), power(P_i), energy harvested by the turbine in each dive/ascent cycle (E_{h_i}) using Eq.13.

$$E_{h_i} = P_i * d_w * 2/V_i \quad (13)$$

Step 13: Input the V_i to the hull resistance function in step (6), then, the mathematical model will calculate the resistance of the hull R_{h_i}. Followingly, the total resistance (R_{t_i}) of the hull and turbine can be calculated by Eq.14.

$$R_{t_i} = R_{h_i} + T_{t_i} \quad (14)$$

Step 14: Determine the actual operating speed of the glider by force balance analysis. From step (10) to step (14), the math model will

calculate different velocities until it finds the velocity V_x when $R_t = ballast\ force$. This velocity V_x is the operating speed of the system. Then the mathematical model will output this V_x and corresponding Cp_x, Ct_x, T_{t_x},P_x, E_{h_x} and the turbine geometry.

Step 15- Step 18: When all operating TSR, design TSR, and design radius are calculated, the mathematical model will output the optimum turbine geometry with the highest harvested energy(E_h).

THE RESULT AND ANALYSIS OF THE MATHEMATICAL MODEL

An Optimal Turbine

As mentioned above, the mathematical model can be used to determine the optimal turbine geometer for the energy harvest mechanism. Shown as Fig.14, the mathematical model can output the energy harvested by the energy harvest mechanism in one power generation cycle (E_h) when different design TSRs and radiuses are used. Each grid point in Fig.14 contains a turbine geometry, the turbine geometry with the highest E_h is the optimal turbine designed by the whole mathematical model.

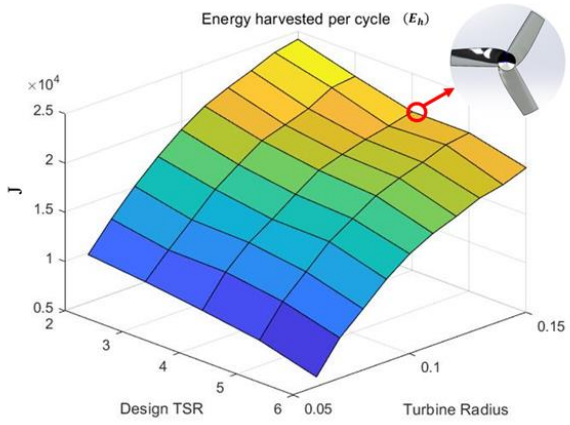

Fig.14 energy harvested by different turbine geometries

The Guiding Significance Of Mathematical Model For Turbine Design

The mathematical model can also be used to guide the design of the turbine in this study. From Fig.14, the trend can be observed that the energy yield increases with the increase of radius and the decrease of the design TSR.

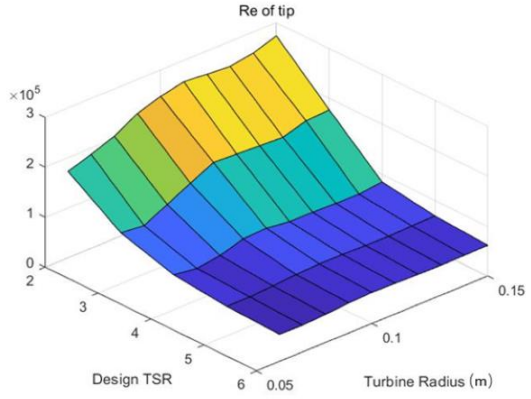

Fig.15 the Re of different turbines

The reason why the energy yield increases as the radius increases is that the thrust of the turbine tends to increase with the increase of the radius. During the entire energy harvesting process, the turbine keeps competing with the glider hull for energy, the turbine with a higher thrust can win more energy in the competition. The reason why the energy decreases as the design TSR increases is that the Reynolds number of the turbine will drop into a low Re range where the hydrodynamic performance of the turbine will deteriorate when the design TSR increases. Fig.15 shows how the working Reynolds number at 0.9 R of different turbine blades change with different turbine radii and design TSRs. So, the conclusion can be made that the large radius and the low design TSR should be selected within the allowable range in the turbine design in this study.

The mathematical model also shows the ratio of Cp to Ct (Cp/Ct) is the key factor for the highest energy yield. Fig,16 shows the relationship of turbines' energy yield (E_h) , the Cp/Ct, the Cp, and the power output in figure (a), (b), (c), (d) respectively in different design TSR and radiuses. Compared to the Cp and the power output of the turbine, the Cp/Ct shows a more similar trend and stronger correlations with the energy yield per working cycle (E_h). The reason is that the design of the turbine differs from traditional tidal turbines as the turbine is essentially driven by the gravity/buoyancy force instead of a moving flow and the turbine have to keep competing with the hull for energy in the power generation mode, the key to maximizing the E_h is the balance between Cp and Ct. In this case, a higher Cp/Ct can lead to a higher energy yield. Therefore, we can get the conclusion that the turbine should pursue higher Cp/Ct rather than higher Cp or power output in the design process. The math model will be further developed according to the conclusion. However, the conclusion may change in other cases when the glider hull with higher Ct is selected in the mathematical model, a glider hull with a higher Ct will get more energy when competing with a turbine for energy, resulting in a decrease in the energy yield of the turbine and influencing the optimal Cp/Ct.

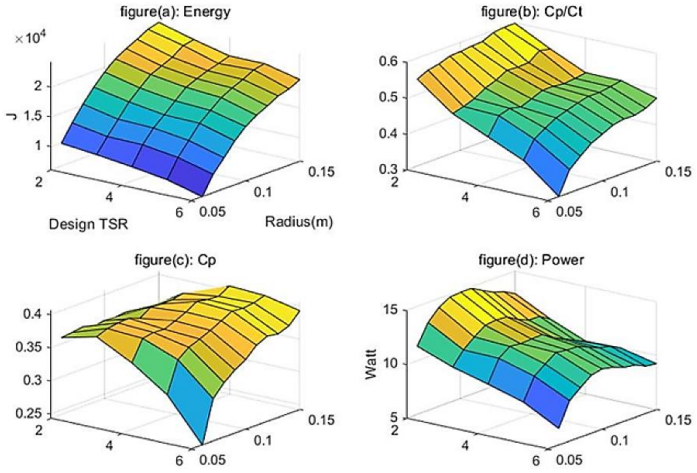

Fig.16 energy yield, Cp/Ct, Cp and power output in (a)(b)(c)(d) respectively

The Power Generation Capacity Of The System

From the result of the math model, we can also see the power generation capacity of the whole system and the significance of its application on the glider in this case. The math model shows that this system can harvest about 24KJ of energy in one dive/ascent cycle in the power

generation mode. Considering that the power consumption of a typical glider of each dive/ascent cycle in gliding mode is about 6kJ of energy(Russ E. Davis, Eriksen, & Jones, 2002; Falcão Carneiro & Gomes de Almeida, 2018), it can be estimated that the energy harvested by the energy harvest system in 1 cycle in the power generation mode can support the energy consumption of the glider in 4 cycles in the gliding mode. As mentioned above, the ballast force of the thermal buoyancy engine is 25 N, and the working length of the buoyancy engine in one cycle is 2000 meters, it can be concluded that the thermal buoyancy engine outputs 50kJ of energy in one cycle. Considering that the system can harvest about 24kJ of energy in one dive/ascent cycle, it can be concluded that the energy conversion efficiency of the power generation system is about 48%.

CONCLUSION

This work investigates a new-type energy harvesting mechanism applied to the glider. The energy harvesting mechanism can use a thermal buoyancy engine and a turbine behind the hull to harvest energy.
To maximize the energy yield of the mechanism, this paper develops a new-type thermal buoyancy engine with patent applied, the new-type thermal buoyancy engine can fully use the pressure that the phase change material can generate (PCM) and amplify the ballast capacity to provide more kinetic energy to the turbine without increasing the mass of PCM.

To optimize the turbine for harvesting the highest energy, a mathematical model is established based on the BEM theory which has been modified according to the wake distribution and Reynolds number. The mathematical model can output an optimized turbine and its corresponding energy yield in one cycle. The mathematical model also shows the trend that the energy harvest by the turbine will increase with the decrease of the design TSR and the increase of the turbine radius. And the mathematical model shows that the turbine should pursue higher Cp/Ct rather than higher Cp or power output in the design process in this case. The conclusions can be a guiding philosophy to further develop the math model to design the optimal turbine.

The result of the mathematical model indicates that the energy harvesting system with 12 liters (about 10kg) of n-pentadecane can harvest 24KJ of energy in each dive/ascent cycle with an energy conversion efficiency of 48%. The 24 KJ of energy can support the energy consumption of the glider in 4 cycles in the gliding mode, which indicates that the energy harvesting system can make the gliders forever ocean resident.

Nevertheless, it should be pointed out that the hydrodynamic interaction between the hull and the turbine, and the motion of the hull in six degrees of freedom have not been considered in the math model yet. They will be implemented in future work based on CFD simulation.

REFERENCES

Bangga, G., Hutomo, G., Syawitri, T. P., Kusumadewi, T. V., Oktavia, W., Sabila, A., Setiadi, H., Faisal, M., Hendranata, Y., Lastomo, D., Putra, L., Kristiadi, S. R., & Bumi, I. M. (2018). Enhancing BEM simulations of a stalled wind turbine using a 3D correction model.

Buhl, M. L. (2005). New Empirical Relationship between Thrust Coefficient and Induction Factor for the Turbulent Windmill State.

Chaviaropoulos, P. K., & Hansen, M. (2000). Investigating Three-Dimensional and Rotational Effects on Wind Turbine Blades by Means of a Quasi3D Navier-Stokes Solver. *Journal of Fluids Engineering-transactions of The Asme - J FLUID ENG, 122*.

Chao, Y. (2016). Autonomous underwater vehicles and sensors powered by ocean thermal energy. OCEANS 2016 - Shanghai.

Davis, R. E., Eriksen, C. C., & Jones, C. (2002). Autonomous Buoyancy-Driven Underwater Gliders.

Davis, R. E., Eriksen, C. C., Jones, C. P. J. T. t., & vehicles, a. o. a. u. (2002). Autonomous buoyancy-driven underwater gliders. In (pp. 37-58): Taylor and Francis, London.

Deters, R., Ananda, G., & Selig, M. (2014). Reynolds Number Effects on the Performance of Small-Scale Propellers.

Eriksen, C. C., Osse, T. J., Light, R. D., Wen, T., Lehman, T. W., Sabin, P. L., Ballard, J. W., & Chiodi, A. M. (2001). Seaglider: a long-range autonomous underwater vehicle for oceanographic research. *IEEE Journal of Oceanic Engineering, 26*(4), 424-436.

Falcão Carneiro, J., & Gomes de Almeida, F. (2016). Model of a thermal driven volumetric pump for energy harvesting in an underwater glider. *Energy, 112*, 28-42.

Falcão Carneiro, J., & Gomes de Almeida, F. (2018). Model and simulation of the energy retrieved by thermoelectric generators in an underwater glider. *Energy Conversion and Management, 163*, 38-49.

Javaid, M., Ovinis, M., Nagarajan, T., & Hashim, F. (2014). Underwater Gliders: A Review. *MATEC Web of Conferences, 13*, 02020.

Jones, C., Allsup, B., & DeCollibus, C. (2014, 14-19 Sept. 2014). *Slocum glider: Expanding our understanding of the oceans.* 2014 Oceans - St. John's.

Klintberg, L., Karlsson, M., Stenmark, L., Schweitz, J.-Å., & Thornell, G. (2002). A large stroke, high force paraffin phase transition actuator. *Sensors and Actuators A: Physical, 96*(2), 189-195.

Kong, Q., Ma, J., & Xia, D. (2010). Numerical and experimental study of the phase change process for underwater glider propelled by ocean thermal energy. *Renewable Energy, 35*(4), 771-779.

Li, L. (2013). Experimental Testing of Low Reynolds Number Airfoils for Unmanned Aerial Vehicles.

Liu, S., & Janajreh, I. (2012). Development and application of an improved blade element momentum method model on horizontal axis wind turbines. *International Journal of Energy and Environmental Engineering, 3*(1), 30.

Ma, Z., Wang, Y., Wang, S., & Yang, Y. (2016). Ocean thermal energy harvesting with phase change material for underwater glider. *Applied Energy, 178*, 557-566.

Ragheb, M., & Ragheb, A. M. (2011). Wind turbines theory-the betz equation and optimal rotor tip speed ratio. *Fundamental and advanced topics in wind power, 1*(1), 19-38.

Shen, W. Z., Mikkelsen, R., Sørensen, J., & Bak, C. (2005). Tip loss correction for wind turbine computations. *Wind Energy, 8*, 457-475.

Sherman, J., Davis, R. E., Owens, W. B., & Valdes, J. (2001). The autonomous underwater glider "Spray". *IEEE Journal of Oceanic Engineering, 26*(4), 437-446.

Shi, W., Hou, H., Xu, Y., & Mehmet, A. (2022). A new thermal buoyancy engine and its control method. *Intellectual Property Office,* GB2597095.

Wang, G., Yang, Y., & Wang, S. (2020). Ocean thermal energy application technologies for unmanned underwater vehicles: A comprehensive review. *Applied Energy, 278*, 115752.

Webb, D. C., Simonetti, P. J., & Jones, C. P. (2001). SLOCUM: an underwater glider propelled by environmental energy. *IEEE Journal of Oceanic Engineering, 26*(4), 447-452.

Yang, Y., Wang, Y., Ma, Z., & Wang, S. (2016). A thermal engine for underwater glider driven by ocean thermal energy. *Applied Thermal Engineering, 99*, 455-464.